SOLDER-JOINT RELIABILITY OF A 0.65MM PITCH MOLDED ARRAY PACKAGE FOR AUTOMOTIVE APPLICATIONS

Burton Carpenter, Mollie Benson, Andrew Mawer
NXP Semiconductors, Inc.
TX, USA
Burt.Carpenter@nxp.com, Mollie.Benson@nxp.com, Andrew.Mawer@nxp.com

ABSTRACT
BGA components used in high reliability automotive microprocessor applications have historically been 0.8mm pitch or larger. Recently, emerging market requirements have pushed BGA pitches down to 0.65mm. However, industry expectations of solder-joint reliability remain constant; customers expect cyclical thermal fatigue lifetimes to be the same as, or in some cases more robust than prior generations of packages. In addition, automotive Tier 1 electronics manufactures often include drop test and other board mounted testing criteria to mitigate the risk of module level failure during SMT, module or final vehicle assembly.

The paper reports the board level reliability of a 0.65 pitch, 10x10mm MAPBGA (molded array plastic BGA) package used as an automotive radar microprocessor. Thermal fatigue life was assessed per IPC-9701A using AATS (air-to-air thermal shock) between -40ºC and +125ºC, while drop testing followed the JEDEC JESD22-B111A at 1500G's.

Six package configurations were studied: each combination of two package BGA pad surface finishes (Ni/Au and OSP [organic solderability preservative]) and three package solder ball alloys (SnAg, SAC405, and SAC-Bi [a Bi containing SAC derivative]). PCB variables included pad diameter, and the effect of interstitial through vias in the BGA footprint. The solder-joint lifetimes from the AATS tests were observed to depend on the package variables, with Ni/Au BGA pads performing better than the OSP pads. The PCB variables were not significant. By contrast, the OSP BGA pad finish had better drop test performance.

Key words: BGA, Solder-joint reliability, SnAg, SAC, temperature cycle, thermal fatigue, drop, OSP

INTRODUCTION

A variety of factors influence the decision to choose a particular pitch for a BGA package, including package size, package substrate routability, package cost, PCB footprint, PCB routability and layer count, PCB cost, and SMT process capability and yield. Automotive AEC Grade 1 [1] applications have long used 0.8mm pitch or greater as the optimum compromise of these various factors. However, there is a design space where tighter pitches are preferred, namely for smaller packages which need fewer escape routes on the PCB. This is the case for the radar microprocessor under investigation here.

While the primary objective of this study was to baseline the solder-joint thermal fatigue life for the POR (plan of record) package, drop test data was also collected since automotive electronics manufactures often include drop test criteria to mitigate the risk of module level failure during SMT, module or final vehicle assembly.

Several factors were investigated to understand their influence. First was the component BGA pad finish. While electroplated Ni/Au is the standard for fatigue life sensitive applications, OSP can improvement drop test performance [2, 3]. The objective here was to quantify this trade-off on the package of interest. Secondly, three package BGA solder alloys were investigated: SnAg, SAC405, and SAC-Bi (compositions given in Table 1). SnAg has been shown to have better temp cycle and tray drop reliability [4-8], though SAC405 is more common in the industry. A variety of Bi containing alloys are now available by from solder ball suppliers. These are generally stiffer with higher modulus than SnAg or higher Ag SAC alloys, and have found success by other investigators [9, 10].

In temperature cycling, there were two PCB variables. PCB pad diameters were 0.325mm (50% of pitch) and 0.300mm. Past experience showed that the slightly smaller diameter was more reliable in cycling provided the failure location remained on the package side of the solder-joint [11]. Lastly, the effect of dummy mechanical through-vias interstitial to the BGA pads was investigated. IPC-9701A [12] requires these "to approximate mechanical effect of vias on product PWBs". The experimental matrix is summarized in Table 2.

The focus of this paper is to show that 0.65mm pitch BGA can pass auto grade temperature cycling requirements, and report how package and PCB variations may affect the result.

EXPERIMENTAL METHODS

Package Design

The component details are summarized in Table 1; the two variables are highlighted in yellow. Note the die is fairly large in this package. The schematic in Figure 1 and cross-section in Figure 2 show it extending nearly to the last BGA row on the west and east sides. SRO (solder resist opening) and solder sphere diameter should be designed at 50% of the BGA pitch (or slightly larger) to maximize solder-joint

reliability (non-automotive applications have employed 0.300mm SRO with 0.300mm diameter solder balls for improved substrate routability). An assessment of the temperature cycle lifetime for these non-automotive components indicated the 141MAPBGA would not meet the requirement (1500 cycles before first failure with sample size ≥30) unless these features were increased. Therefore, the SRO/sphere combination 0.325mm/0.330mm was selected.

Other factors are typical for a MAPBGA (molded array plastic BGA) package, including the mold cap covering of the entire substrate top surface. The substrate design had pair-wise connections on the bottom metal (M2) between BGA pads that enabled a daisy-chain electrical monitor of the solder-joints during cycling.

Table 1. Package Characteristics

Parameter	Value
Body Size	10mm x 10mm
IO Count	141
BGA Pitch	0.65 mm
Mold Size	10mm x 10mm
Mold Thickness	0.8mm
Mold Material	Epoxy Mold Compound α1=9ppm/°C E=26GPa Tg=125°C (TMA)
Substrate Thickness / # Layers	0.30mm / 2L
Substrate Material	α1=16ppm/°C E=19GPa Tg=180°C (TMA)
Die Size	6.12mm x 6.92mm
Die Thickness	0.280mm
Package Pad (SRO)	0.325mm SMD
Pad Finish	Variable: Electroplated Ni/Au, OSP
Sphere Diameter	0.330mm
Sphere Alloy	Variable: SnAg*, SAC405**, SAC-Bi***

* 96.5% Sn, 3.5% Ag
** 95.5% Sn, 4.0% Ag, 0.5% Cu
*** 92.5% Sn, 4.0% Ag, 0.5% Cu, 3.0% Bi + Ni (trace)

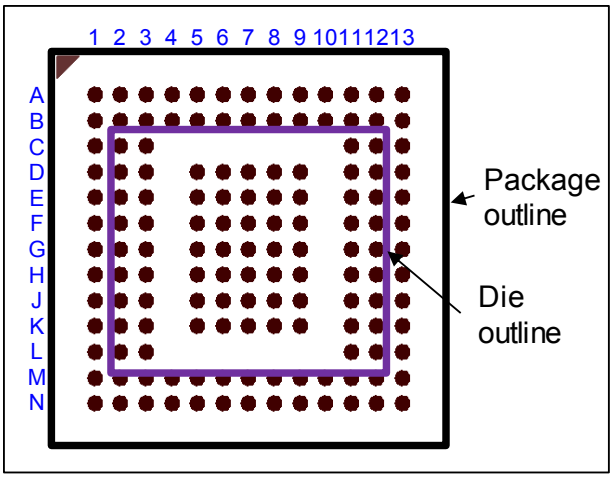

Figure 1. BGA footprint top view.

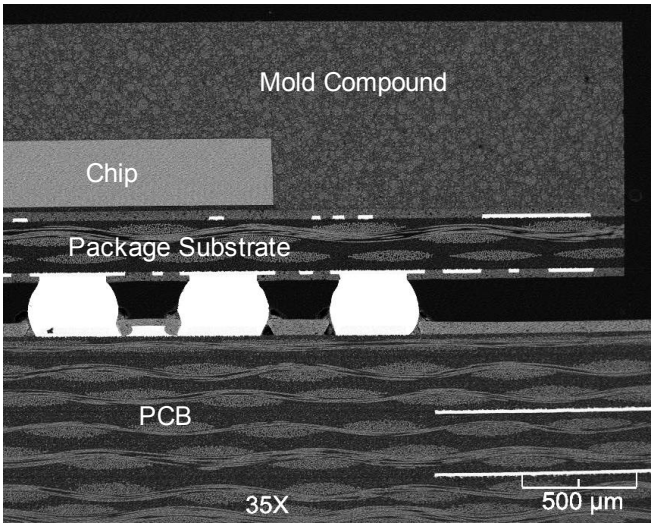

Figure 2. Cross-section of package mounted on AATS PCB.

Table 2. Package and PCB combinations.

		PCB Configuration			
		Pad ϕ	0.325 mm		0.300 mm
		Via	Interstitial	None	Interstitial
Package Config	Ni/Au	SnAg	1A*	1B***	1C*
		SAC405	2A*	2B**	
		SAC-Bi	3A*	3B**	
	OSP	SnAg	4A*	4B***	4C*
		SAC405	5A*	5B**	
		SAC-Bi	6A*	6B**	
	Finish	Alloy			

* AATS only ** Drop only *** Both

PCB Design and Assembly

The PCB and assembly details are in Table 3 with the variables highlighted in yellow. The PCB design connected BGA pads pair-wise in the top metal to complement the package substrate, thus completing the daisy-chain connection as shown schematically in Figure 3. The two footprints used for temperature cycle comparing with and

without interstitial vias are shown in Figure 4. An attempt was made to include dummy interstitial vias wherever functional routing traces were absent. In total 49 dummy vias were added. As recommended by JEDEC, the drop test PCB design included via-in-pad, while the temperature cycle boards did not. Photos of both boards are shown in Figure 5.

Assembly of daisy-chain parts to boards followed industry norms. Solder paste printed to the boards was SAC305 (Sn3.0%Ag0.5%Cu) with Type IV (28 – 40 μm diameter) solder powder and a no-clean flux system. Components were placed on boards using a dual eyepiece placement machine to align parts to the solder-paste print. Finally, boards were run through a 10-zone reflow furnace with a peak temperature between 235°C and 245°C.

Table 3. PCB and SMT assembly details.

Parameter	AATS	Drop
PCB Material	Epoxy Laminate α1=12ppm/°C E=24GPa Tg=180°C (TMA)	
PCB Thickness	1.4 mm, 8 layer	1.0mm, 10 layer
Via type	Variable: Interstitial , None	Via in pad
PCB Pad Diameter	Variable: 0.300mm, 0.325mm	0.325mm
PCB Pad Finish	OSP	
Stencil	Aperture matched Pad Diameter Thickness 0.100mm	
Stencil Finish	Laser cut openings with electropolish and Ni coating	
Paste	SAC305, No clean, Type IV powder	

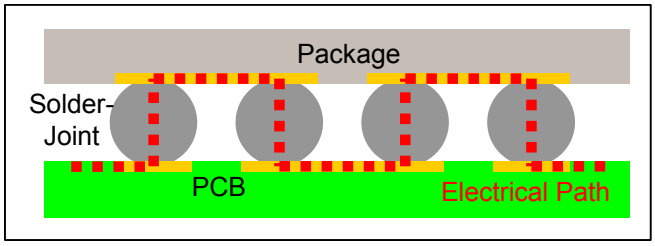

Figure 3. A daisy-chain connection representation between package substrate bottom metal and PCB top metal. The red dashed line illustrates the electrical path.

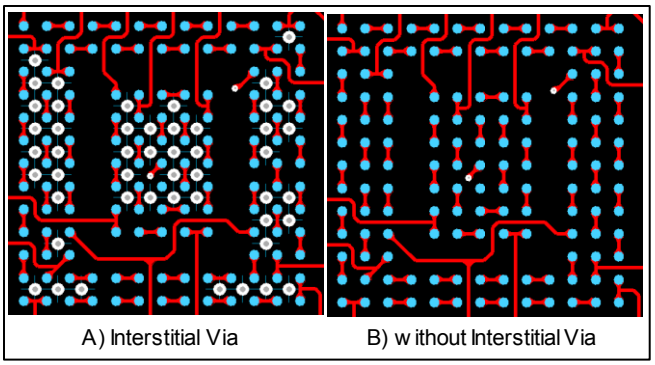

Figure 4. BGA footprints. The "A" set had non-functional mechanically drilled vias added to the BGA pad interstitials. (Blue circle = BGA pad, White circle = Via pad)

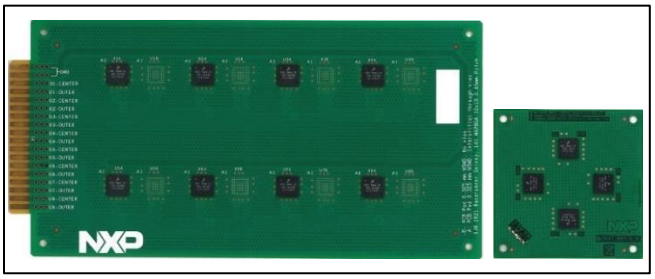

Figure 5. Thermal Shock (left) and JEDEC Drop (right) PCBs. Images Not to Scale.

Temperature Cycle Test Method

Assemblies were tested in an Air-to-Air Thermal Shock (AATS) dual chamber system whereby one chamber remained hot (+125°C) and the other remained cold (-40°C). An elevator system moved test boards between these chambers within about 10 seconds.

Both chamber dwell times were set at 30 minutes totaling 1 cycle/hour. Typically, ~5 minutes was required to reach equilibrium, yielding ~25 min dwells. Figure 6 displays a typical temperature profile obtained by placing thermocouples in the solder-joints.

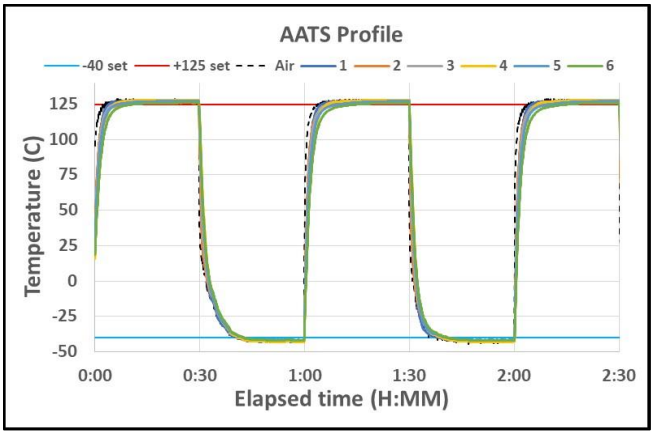

Figure 6. AATS temperature profile.

Assemblies were monitored in-situ during cycling using a 1.2mA current through each net. An event detector logged a failure when a net resistance exceeded 300 ohms. Failures

were defined per IPC-9701A [12] and were recorded and analyzed on a by-unit basis (a unit failed when any solder-joint failed.) For each test cell, cycling continued until at least 75% of the samples failed, after which the data were fit to 2-paramter Weibull distributions using MLE (maximum likelihood estimate). Comparisons were done based on first failure and characteristic life (Eta).

Drop Test Method

Drop testing was completed per JEDEC JESD22-B111A condition B [13]. Drop heights were typically 41cm to achieve 1500G with a 0.5ms duration, half-sine pulse. During set-up, PCB strain was measured with a rectangular rosette strain gauge to be approximately 1300μstrain max. Testing was completed to 75% failure or to 300 drops, whichever occurred first.

Solder Ball Shear

Ball shear on representative components was performed to ensure proper attach during the package assembly process to and characterize the attached solder ball strength. Low speed (280um/sec) shear tests were done to characterize bulk solder strength following JEDEC JESD22-B117B [14].

Cross-section

Mechanical sectioning was used to characterize the solder-joints immediately after board mount, crack propagation study and failure analysis (FA). Standard potting, sectioning, grinding and polishing techniques were used to prepare the samples. SEM images were captured for the study and joint measurements. In all cases, sections were made through the joint center line. One caution: crack front propagation may be at any arbitrary angle to the cross-section plane, thereby distorting crack length measurements.

Dye-and-pry

Dye-and-pry was a quick and simple method to obtain an overall view of joint cracking quantity, degree and distribution. A dye was applied to the solder-joint array to mark crack locations, followed by a forced separation of package from board. Cracks formed during cycling became stained with ink and were distinguishable from fracture surfaces created because of the forced pry [15]. Note that PCB pads often ripped out during peel, even when solder-joint cracking had occurred. In these incidences, it was assumed the degree of cracking was low (<50%) because the solder-joint strength was greater than PCB pad adhesion.

EXPERIMENTAL RESULTS

Experimental Matrix

Six combinations of daisy-chain packages were assembled from the two substrate surface finish types and three solder ball alloys. These are listed down the left side of Table 2 and designated sequentially 1-6. A letter is appended to the cell name depending on which PCB it was assembled on. For example, cell 1A is package type 1 (Ni/Au with SnAg) assembled on PCB type A (0.325mm PCB pad with interstitial mechanical via. Note that only partial matrices were built for both cycling (10 cells) and drop (6 cells). Also recall that the drop test PCB had via-in-pad while the cycling board did not.

Characterization

The ball shear distributions are graphed in Figure 7. Cells 1-5 exhibited purely mode 1A failure (ductile) while the OSP/SAC-Bi combination was mixed between 1B (Quasi-Ductile) and 4B (Quasi-Brittle). (Mode definitions per [14]). While all packages were well above the lower spec limit of 250g, the differences can provide insight. The higher modulus of the SAC-Bi enabled higher shear strength values for Cell 3 on Ni/Au. However, the mixed failure mode on OSP minimized the difference since the brittle mode failures had generally lower strength.

Figure 8 shows examples of as-assembled solder-joints. Slight non-wetting was observed on about 50% of the solder-joints in the OSP cells, as can be seen in the higher mag images of Figure 9. With all three alloys, small non-wet spots indicated possible areas of OSP damage. While the root cause was not positively identified, it is likely that a tool tip touched the substrate pads at some point prior to ball mount. For SAC-Bi (Cell-6), some edge non-wetting was also observed and believed to be caused by a non-optimized flux process. The equivalency of the ball shear results between Cells 1, 2, 4 and 5 (Figure 7) indicate that the non-wetting area was not significant for the SnAg and SAC405 alloys.

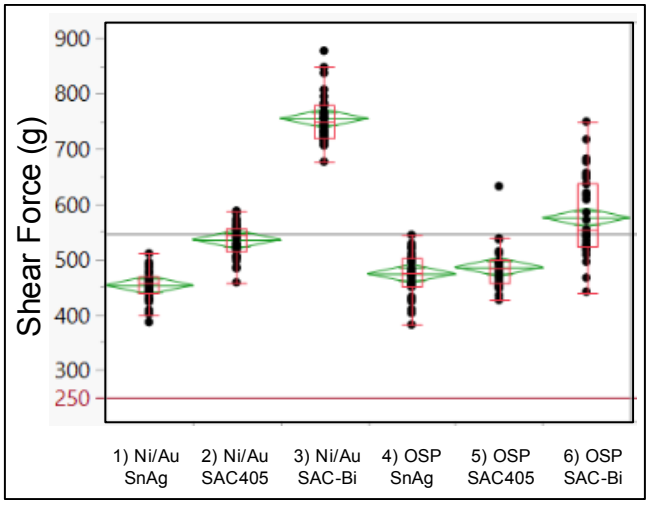

Figure 7. Ball shear distributions.

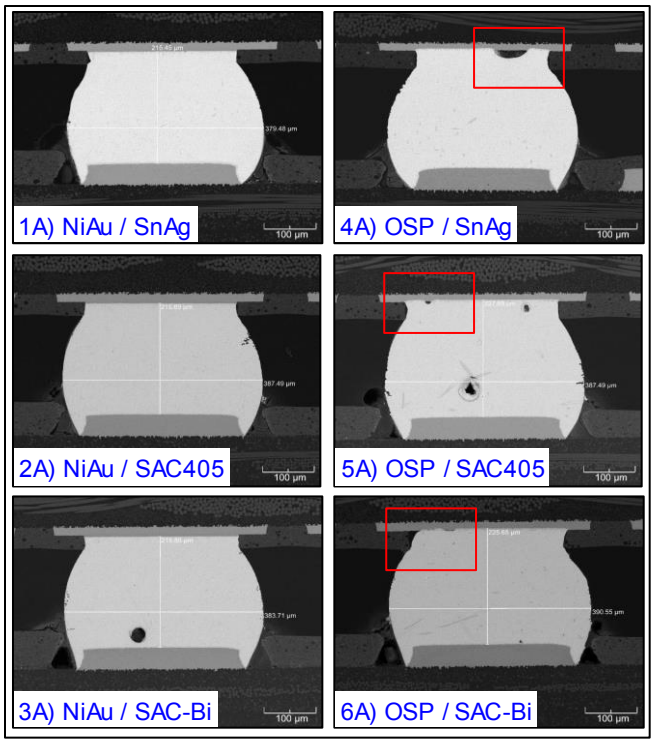

Figure 8. Example solder-joints after board mount before cycling. All OSP cells showed non-wetting on package side.

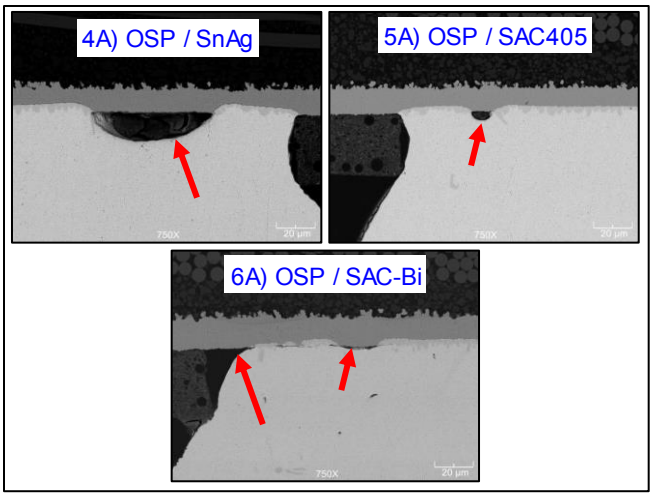

Figure 9. High mag images of non-wetting on OSP.

Temperature Cycle Test Results and Failure Analysis

Cycling results for the 10 cells are summarized in Table 4. For clarity of presentation, these are plotted on three different Weibull charts to highlight various comparisons.

Figure 10 plots all six package types for a common set of PCB variables (0.325mm pad diameter with interstitial vias). The Ni/Au groups outperformed the OSP ones. In fact, the OSP lifetimes did not meet the performance targets for this application (1500 cycles to first failure). The effect of alloy was more subtle. Consistent with prior investigations [4-8], the fatigue lifetime of SnAg was longer than SAC405 on either pad finish. SAC-Bi, while better than either SnAg or SAC405 on OSP, gave mixed results on Ni/Au. The Ni/Au SAC-Bi first failure was earlier than either of the other alloys, but due to the lower beta, the characteristic lifetime was higher.

Table 4. Summary of temperature cycle results

Cell	Package Pad Type	Solder Ball Alloy	PCB Pad (mm)	Via Type	n	Beta	Eta	1st Fail
1A	NiAu	SnAg	0.325	Interstitial	34	9.8	2442	1651
1B	NiAu	SnAg	0.325	None	16	13.4	2361	1970
1C	NiAu	SnAg	0.300	Interstitial	34	9.3	2457	1690
2A	NiAu	SAC405	0.325	Interstitial	19	12.7	1968	1576
3A	NiAu	SAC-Bi	0.325	Interstitial	18	3.8	3697	1443
4A	OSP	SnAg	0.325	Interstitial	17	6.4	1123	736
4B	OSP	SnAg	0.325	None	14	5.2	1086	570
4C	OSP	SnAg	0.300	Interstitial	11	5.9	1092	653
5A	OSP	SAC405	0.325	Interstitial	19	4.4	1103	509
6A	OSP	SAC-Bi	0.325	Interstitial	14	4.8	2165	1138

Failure analysis shown in Figures 11 and 12 provides further insight. Both SnAg and SAC405 cracks formed in the bulk solder just near the package side interfacial IMC. However, most cracks in the SAC-Bi joints were typically brittle failure in or along the package side IMC layers. Indeed, some were not, and this mix of failure modes likely

contributed to the larger spread in cycles to failure. Also evident in these images is the propensity for solder-joints near the die shadow perimeter to fail first, which is typical for smaller packages with relatively large die.

PCB variables effects are plotted in Figures 13 and 14, which were all examined using the SnAg solder ball. Removing the interstitial vias (Figure 13) caused no significant change in cyclic fatigue life. Likely these had no impact on board stiffness as was hypothesized. Likewise, the PCB pad diameter had no effect (Figure 14). These results differs from the previous investigation [11] which found a strong dependence resulting from differences in stand-off height.

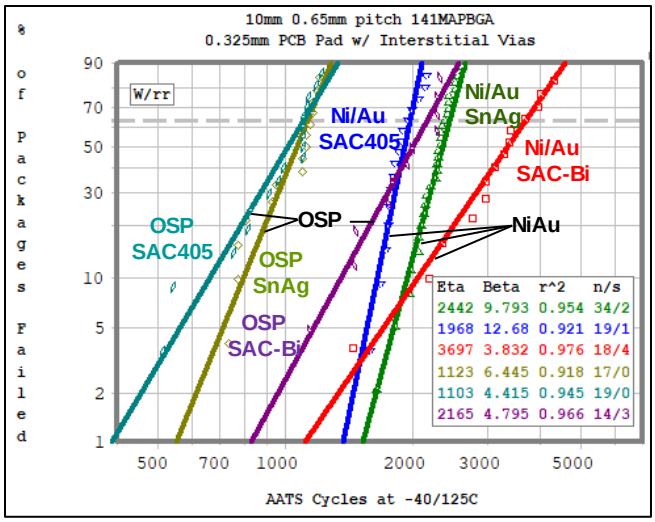

Figure 10. Temp Cycle Weibull plots comparing package pad finish and BGA alloy for packages with 0.325 PCB pads and interstitial vias. (Cells 1A, 2A, 3A, 4A, 5A, 6A)

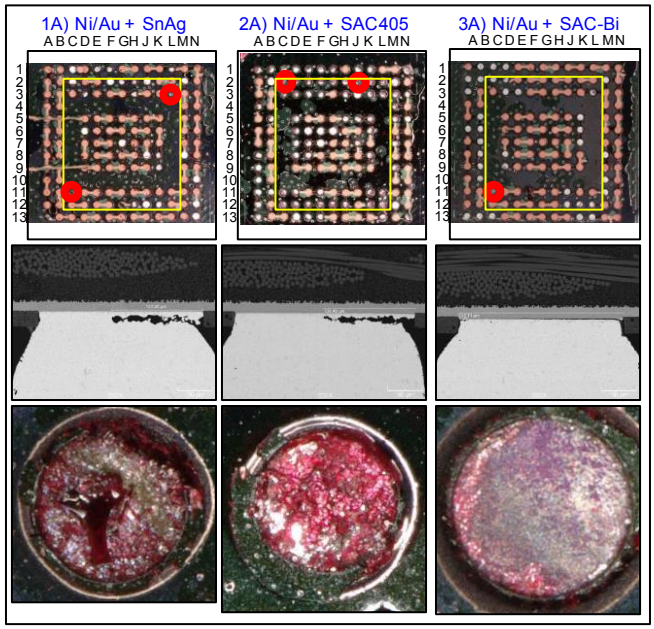

Figure 11. Crack propagation analysis after temperature cycle for Ni/Au cells. Cross-section images all after 1576 cycles. Dye-and-pry photos after 1651 cycles (SnAg first failure), 1576 cycles (SAC405 first failure), 1433 cycles (SAC-Bi first failure). The Bi containing alloy shows brittle IMC fracture.

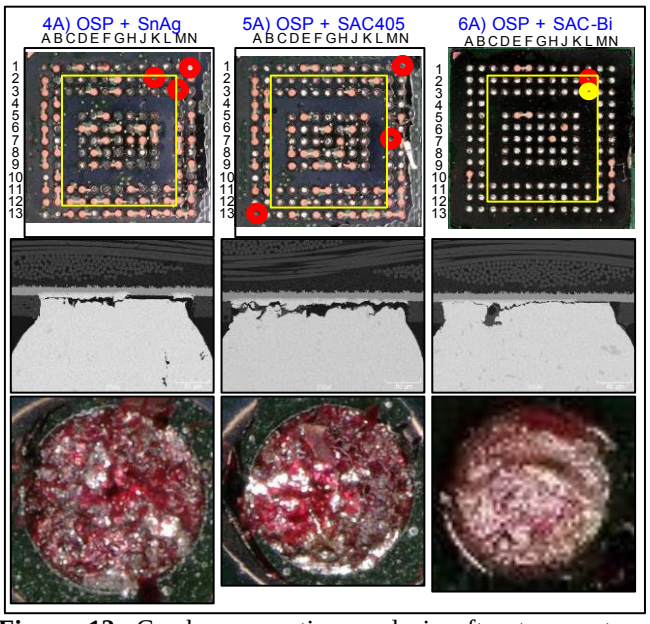

Figure 12. Crack propagation analysis after temperature cycle for OSP cells. Cross-section images all after 1576 cycles. Dye-and-pry photos after 952 cycles (SnAg sixth failure), 985 cycles (SAC405 eight failure), 2146 cycles (SAC-Bi ninth failure). The Bi containing alloy shows brittle IMC fracture.

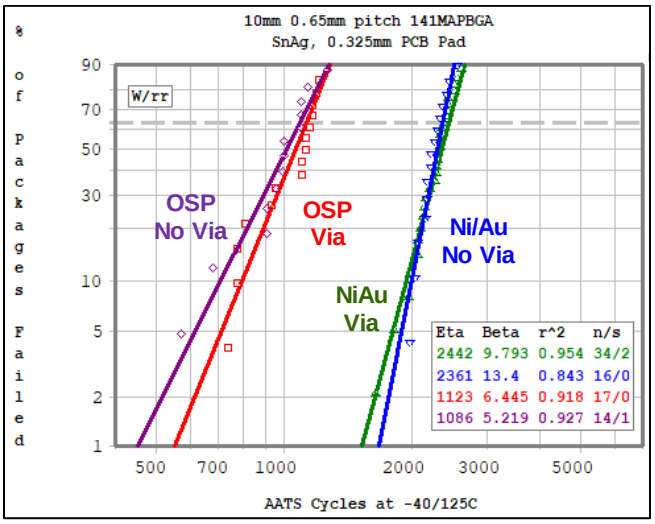

Figure 13. Temp Cycle Weibull plots comparing package pad finish and PCB via configuration for SnAg BGA solder ball alloy and 0.325 PCB pads. (Cells 1A, 1B, 4A, 4B)

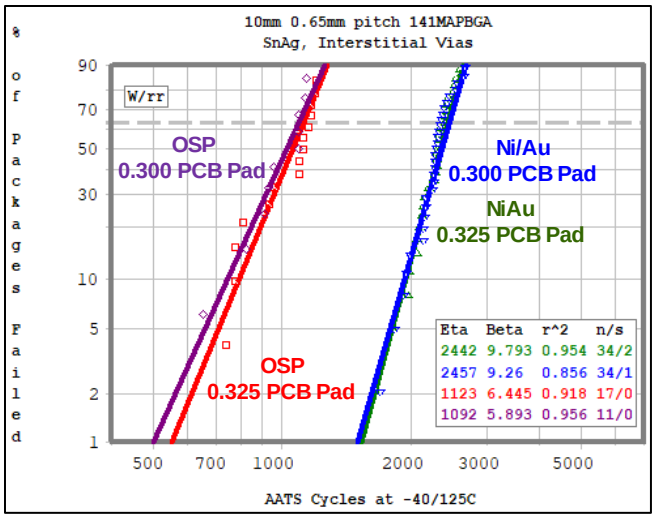

Figure 14. Temp Cycle Weibull plots comparing package pad finish and PCB pad diameter for SnAg BGA solder ball alloy and interstitial PCB vias. (Cells 1A, 1C, 4A, 4C)

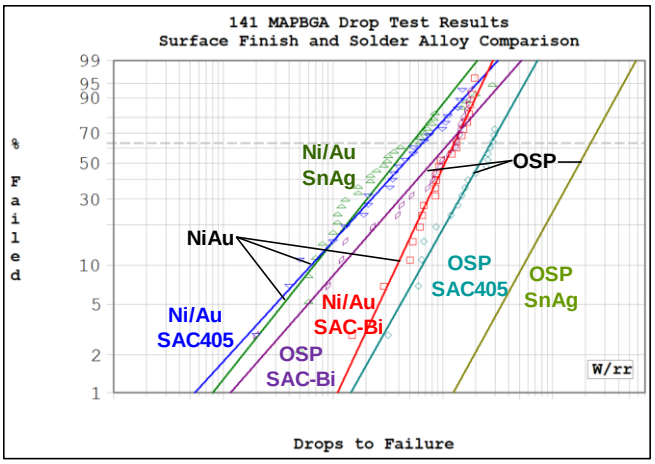

Figure 15. Drop Test Weibull plots comparing package pad finish and BGA alloy for packages (Cells 1B, 2B, 3B, 4B, 5B, 6B). The line for Cell 4 (OSP, SnAg) is a lower boundary estimate since there were no failures after 300 drops.

Drop Test Results and Failure Analysis

Contrary to temperature cycle, the cells with OSP surface finish outperformed the Ni/Au cells in drop test. Figure 15 shows the Weibull plots. Since the OSP/SnAg cell did not have any recorded electrical failures, a line was plotted using an estimated Beta and presumed first failure on the subsequent drop. SnAg and SAC405 alloys were clearly better on OSP. While SnAg was better than SAC405 with OSP, they were nearly identical on Ni/Au. The SAC-Bi had similar characteristic lifetimes on the different surfaces, but earlier first failures, likely caused by the non-wetting during sphere attach.

The cross-sections shown in Figure 16 provides more insight. Except for SnAg on OSP (Cell 4B, which had no failures) samples were sectioned soon after the failure occurred.

Brittle fractures propagated in the interfacial IMC layer package side for the five failed samples. The OSP/SnAg sample that did not fail had a bulk solder crack initiation near the package side. Corner solder-joints failed before others in the array. Additional FIB cross-sections were completed on drop test failures to understand the effect of the surface finishes and their roles in the mode of fracture propagation. The fracture Cell 1B (SnAg on Ni/Au) shown on the left side of Figure 17 separated the IMC layer from the Ni.

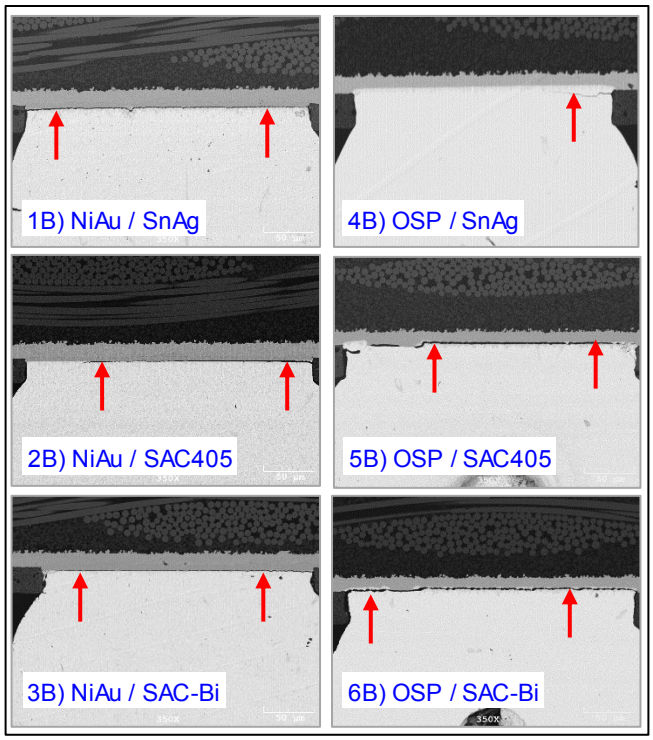

Figure 16. Crack propagation analysis for drop cells. OSP with SnAg (cell 4B) depicts bulk solder-joint cracking near the package, all others have fractured in the package side interfacial IMC. SEM taken after failure, except for cell 4B which had no failures. All are corner solder-joints.

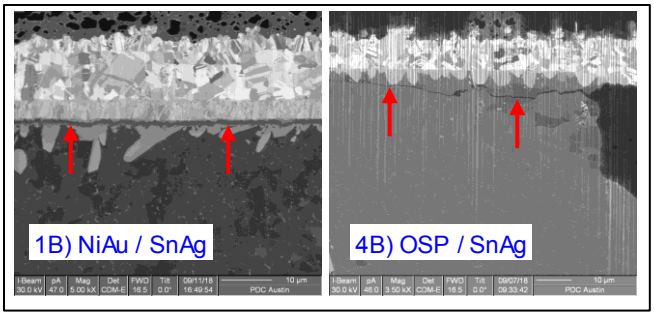

Figure 17. Ion beam images of cracks formed in SnAg samples after drop.

DISCUSSION

The primary results of this investigation demonstrated that package pads with Ni/Au finish outperformed OSP in temperature cycle but was inferior in drop. Investigations by other have shown better drop results on package OSP pads. Examples include Kim and Kim [2] for a 0.4mm pitch BGA with low Ag alloys, and Yeh et al. for both high and low Ag alloys [3].

These results are due to the different IMC compositions formed at the OSP (e.g., Cu_6Sn_5) and the Ni/Au (e.g., Ni_3Sn_4) interfaces. However, Figures 8 and 9 show that package side point non-wetting was observed on the OSP cells, plus additional edge non-wetting on the OSP with SAC-Bi balls. It is unknown if the cycling differences result from these non-wets or are intrinsic. Subsequent to this study, improvements in the ball attach assembly process demonstrated higher yields without non-wetting. Thus, a new set of packages were built for the purpose of verifying the result. These will go through temperature cycling and drop testing. Additionally, microstructure studies are in progress on samples from the current study.

Consistent with prior studies [4-8] SnAg solder balls had slightly better cyclical fatigue lifetime than a similar Cu containing alloy, SAC405 in this case. SnAg was also better in drop, as observed by Chheda et al., [16] and Eu et al., [6]. The stiffer SAC-Bi offered potential improvements that were not realized here. For Ni/Au with SAC-Bi solder, the first failure was earlier than either of the other alloys and the low beta indicates variations (material or process) that reduces predictability of when to expect the first failures.

It is interesting to note that while Sweatman et al., [9] observed better temperature cycle lifetime for Bi containing alloys, Coyle et al., [10] did not notice improve performance. This last study reported a Weibull slope reduction for the Bi alloys as was observed in the present study.

The ball shear data was not useful for predicting solder-joint reliability. The shear force and failure modes were essentially the same for Ni/Au and OSP on the non-Bi alloys despite large differences in cycling lifetime.

The POR package (Ni/Au pad with SnAg ball) met the temperature cycle requirement of 1500cycles before first failure with an increase in SRO/sphere diameters from 0.300mm/0.300mm used in non-automotive product to 0.325mm/0.330mm. SAC405 marginally exceed this value, while SAC-Bi was slightly under. None of the OSP packages were able to meet it.

CONCLUSIONS

Thermal cycle fatigue and JEDEC drop test solder-joint reliability were studied on a 0.65mm pitch 141MAPBGA package through *in situ* monitor of packages mounted on PCBs. The primary conclusions are:

1) The POR package (Ni/Au pad w/ SnAg ball) meets the goal of first failure greater than 1500 cycles using a 0.325mm/0.330mm SRO/Ball Diameter.
2) Packages with BGA pad OSP surface finish were not ready for production, due to solder non-wet, and the inability to meet the temperature cycle requirement.
3) The SAC-Bi alloy was not ready for implementation because the temperature cycle first failure was below target, and the low beta indicate high variability in expected performance.
4) A follow-up study is in progress with improved an improved OSP sphere attach process.

ACKNOWLEDGEMENTS

The authors wish to recognize the support and contribution of Paul Galles who orchestrated the experimental solder-joint reliability work. Also, Jenny Yang and Y.F Wang provided the daisy-chain package. Additionally, Alvin Youngblood, Roy Arldt, Tom Battle, Mike Fuller and Arthur Green performed characterization and FA.

REFERENCES

[1] "Failure Mechanism Based Stress Test Qualification for Integrated Circuits", AEC-Q100 Rev-H, September 2014

[2] G. Kim and D. Kim, 0.4mm Solder Ball Pitch Chip Scale Packaging and Drop Test Performance", SMTA Journal, Volume 20 Issue 4, 2007

[3] K.Y. Yeh et al, "The Investigation of the Performance of Bondability and Solderability on Various Substrate Surface Finishes", 2010 5th International Microsystems Packaging Assembly and Circuits Technology Conference

[4] B. Carpenter, et al, "Design and Material Parameter Effects on BGA Solder-Joint Reliability for Automotive Applications", SMTAI 2014, Rosemont, IL

[5] B. Carpenter and T. Koschmieder, "Solder-Joint Reliability of 0.8mm BGA Packages for Automotive Applications", SMTAI 2015, Rosemont, IL

[6] P.L. Eu, M. Ding, I. Ahmad, "Investigation of Sn3.5Ag and Sn3.8Ag0.7Cu Pb-free Alloys for BGA application on Ni/Au Finish" 2007 IMAPS, San Jose

[7] T. Koschmieder, et al, "Comparing Electronic Component Package Materials and Substrate Vendors for Solder-Joint Reliability Improvements" 2011

SMTA International Technical Conference, Fort Worth
[8] M. Meilunas, A. Primavera, S. O. Dunford, “Reliability and failure analysis of lead-free solder joints”, ECTC 2002
[9] K. Sweatman, et al, "Alternative Strengthening Mechanisms for Lead-Free Solders", SMTAI 2017, Rosemont, IL
[10] R. Coyle, et al, "Thermal Cycle Reliability of a Low Silver Ball Grid Array Assembled with Tin Bismuth Solder Paste", SMTAI 2017, Rosemont, IL
[11] B. Carpenter and B. Yeung, “Solder-Joint Reliability of a Large Body Molded Array Package”, SMTAI 2017, Rosemont, IL
[12] “Performance Test Methods and Qualification Requirements for Surface Mount Solder Attachments”, IPC-9701A, February 2006.
[13] "Board Level Drop Test Method of Components for Handheld Electronic Products", JEDEC JESD22-B111A, November 2016
[14] “Solder Ball Shear”, JEDEC JESD22-B117B, May 2014
[15] T. Burnette and T. Koschmieder, “Solder joint failure analysis: Dye penetrant technique”, http://electroiq.com/blog/2003/01/solder-joint-failure-analysis/
[16] B. Chheda, S.M. Ramkumar and R Ghaffarian, "Thermal Shock and Drop Test Performance of Lead-Free Assemblies with No-Underfill and Corner-Underfill", SMTAI 2009